Fabrication of Fiber Bragg Gratings by Visible Femtosecond Laser for Multi-kW Fiber Oscillator

Hongye Li, Xin Tian, Meng Wang, Xiaofan Zhao, Baiyi Wu, Chenhui Gao, Hao Li, Binyu Rao, Xiaoming Xi, and Zefeng Wang

***Abstract*—In this paper, we fabricate a pair of fiber Bragg gratings (FBGs) in large mode area double cladding fiber (LMA-DCF, core/inner cladding diameter: 20/400 μm) by visible (515 nm) femtosecond laser and phase mask for the first time to the best of our knowledge. Then this pair of FBGs are utilized to construct a high power fiber oscillator operated near 1080 nm. The maximum output laser power is more than 3.2 kW with a slope efficiency of ~77.9%, and the beam quality factor M^2 is about 1.28. The FBGs are simply fixed on water-cooling plate without any special package, and the temperature of the FBGs is about 40 °C at the maximum output power. Our research work confirms the reliability of visible femtosecond laser in fabrication of FBGs intended to be applied in high power fiber oscillators.**

***Index Terms*—Fiber Bragg grating, femtosecond laser, oscillator.**

I. Introduction

RECENTLY, high power all-fiber oscillators have been largely applied in industry, material processing and national defense area for their compact structure, resistance to back-propagating light and simple operation [1]. After the first report of kW-level all-fiber oscillator by Alfalight company in 2012 [2], the output power of oscillator increased step-by-step. In 2016, Fujikura company realized a 2 kW all-fiber oscillator using their home-made DCFs with an effective core area of 400 μm^2 [3]. In 2018, national university of defense technology and Fujikura company successively reported single mode 5 kW-level all-fiber oscillators [4], [5]. In 2020, the maximum output power scaled up to 8 kW [6]. By suppressing limited factors like stimulated Raman scattering (SRS) effect [7], [8] and transverse mode instability (TMI) effect [9], [10], the maximum output power is believed to grow up continuously in the future.

Fiber Bragg gratings (FBGs) [11] are indispensable devices in oscillators, which play the role of cavity mirror and realize power output. Ultraviolet exposure [12] is the most common method to fabricate FBGs applied in oscillators. Using this method, the fiber to be inscribed should be hydrogen loaded in advance and thermal annealing is unavoidable after grating inscription [13], [14]. These processes are often time-consuming, moreover thermal annealing may deteriorate the quality of FBGs and cannot eliminate all the hydrogen in the fiber, which results in a heating of FBGs if applied in fiber oscillators. Femtosecond laser is another solution for the fabrication of FBGs. Femtosecond laser direct writing technique has been proved to be effective for FBGs inscription [15]–[18], however, the FBGs by this method are often with high insertion loss, which prevents them from applying in high power laser systems [19], [20]. Femtosecond laser together with phase mask can also fabricate FBGs with high quality just like ultraviolet exposure method [21], [22]. Contrary to ultraviolet exposure method, photosensitivity of the fiber to be inscribed is not necessary anymore, thus, hydrogen loading and thermal annealing are avoided [23]. Inscription of FBGs with femtosecond laser and phase mask is time-saving and can prevent addition heat load in the condition of fiber oscillators. The relevant research works were carried out by Krämer *et al.* from Friedrich-Schiller-Universität Jena. A 1.9 kW oscillator was realized by inscribed a high reflector (HR) in ytterbium doped fibers (YDFs) in 2019 [24], and the next year, they inscribed HR and low reflector (LR) in LMA-DCFs with core and inner cladding diameter of 20 μm and 400 μm, and then this pair of FBGs played the role of cavity mirrors in a 5 kW oscillator [25]. For most of FBGs inscription using femtosecond laser and phase mask, the wavelength of femtosecond laser is 800 nm (invisible), which makes the inscription not so convenient especially for FBGs with a longer length. Besides, the pulse energy threshold is often high [25] for a relatively lower single phonon energy when using 800 nm femtosecond laser. Thus, FBGs inscription with visible femtosecond laser and phase mask

Manuscript received January 10, 2022; accepted January 12, 2022. Date of publication January 18, 2022; date of current version February 1, 2022. This work was supported in part by the National Natural Science Foundation of China under Grants 11974427 and 12004431, in part by The Science and Technology Innovation Program of Hunan Province under Grant 2021RC4027, in part by the State Key Laboratory of Pulsed Power Laser under Grants SKL-2020-ZR05 and SKL2021ZR01, and in part by the Postgraduate Scientific Research Innovation Project of Hunan Province under Grant CX20200046. *(Corresponding author: Zefeng Wang.)*

Hongye Li, Xin Tian, Baiyi Wu, and Hao Li are with the College of Advanced Interdisciplinary Studies, National University of Defense Technology, Changsha 410073, China, and also with the State Key Laboratory of Pulsed Power Laser Technology, Changsha 410073, China (e-mail: lihongye@nudt.edu.cn; tianxin@nudt.edu.cn; wubaiyi@nudt.edu.cn; csu2nudt@163.com).

Meng Wang, Xiaoming Xi, and Zefeng Wang are with the College of Advanced Interdisciplinary Studies, National University of Defense Technology, Changsha 410073, China, with the State Key Laboratory of Pulsed Power Laser Technology, Changsha 410073, China, and also with the Hunan Provincial Key Laboratory of High Energy Laser Technology, Changsha 410073, China (e-mail: wangmeng@nudt.edu.cn; xixiaoming@nudt.edu.cn; zefengwang@nudt.edu.cn).

Xiaofan Zhao, Chenhui Gao, and Binyu Rao are with the College of Advanced Interdisciplinary Studies, National University of Defense Technology, Changsha 410073, China, and also with the Hunan Provincial Key Laboratory of High Energy Laser Technology, Changsha 410073, China (e-mail: zhaoxiaofan_zxf@nudt.edu.cn; chgao163@163.com; raobinyu@nudt.edu.cn).

Digital Object Identifier 10.1109/JPHOT.2022.3143501

may simplify the fabrication process and provide a lower pulse energy.

In this letter, we inscribed a pair of FBGs using 515 nm femtosecond laser phase mask scanning technique, and then a near single mode 3.2 kW fiber oscillator is constructed with this pair of FBGs. The pulse energy is 255 μJ, which is much lower than other research works [25]. The FBGs is simply fixed on water-cooling plate without special package, and when the output power reaches its maximum, the temperature of FBGs is around 40 °C. The slope efficiency of the oscillator is 77.9% and the intensity of Raman-Stokes light is 33 dB below the laser intensity at the operation of 3231 W. Our research works testify the reliability of visible femtosecond laser in high power fiber laser used FBGs inscription

II. Inscription System and Spectrum Characteristics

Fig. 1(a) demonstrates the schematic of femtosecond laser phase mask scanning system. The wavelength of femtosecond laser is 515 nm, the repetition rate is 1 kHz, and the pulse energy is 255 μJ. For the reason that the femtosecond laser is visible, the alignment process before grating inscription is simplified. We can assess the alignment through diffraction pattern, and no extra device is necessary in this process. Moreover, a shorter wavelength decides a smaller diffraction limit, and energy density can thus increase. A lower pulse energy can be utilized to inscribe FBG comparing with what described in ref [25]. After reflecting by two reflectors, the femtosecond laser passes through a galvanometer, a cylindrical lens, and a phase mask in turns before it finally reaches the fiber to be inscribed (In our experiment, the LMA-DCFs are with a core/inner cladding diameter of 20/400 μm.). Due to the beam diameter is only 3 mm, the beam should be moved along the fiber axis when we inscribe a FBG in centimeter scale, thus a reflector, the galvanometer and the cylindrical lens are set on an electrical moving stage. The phase mask and the fiber to be inscribed keep relatively static. What described in ref [25] was translating fiber and phase mask. The stability requirement and hardware implementation difficulty can be decreased in our inscription system. The focal length of cylindrical lens is 25 mm.

There exist three coupling processes in FBGs with core/inner cladding diameter of 20/400 μm: the self-coupling of LP_{01} mode, the self-coupling of LP_{11} mode, and the mutual coupling between LP_{01} mode and LP_{11} mode. As the size of the focus of femtosecond laser is much smaller than the core diameter, the galvanometer should scan vertically to the fiber axis to expand the refractive index modulation area. In this way, the coupling coefficient of fundamental mode increases and the cross coupling between fundamental mode and LP_{11} mode decreases because of a relative uniform refractive index profile in the core region, which can elevate the threshold of transverse mode instability (TMI) [23], [24]. The chirp rate of phase mask is 0.5 nm/cm and the central pitch of phase mask is 1487.6 nm. The second order FBGs with resonant wavelength near 1080 nm can be inscribed through this phase mask. Mode field adaptors (MFAs) are used during spectrum measurement to avoid intermodal interference.

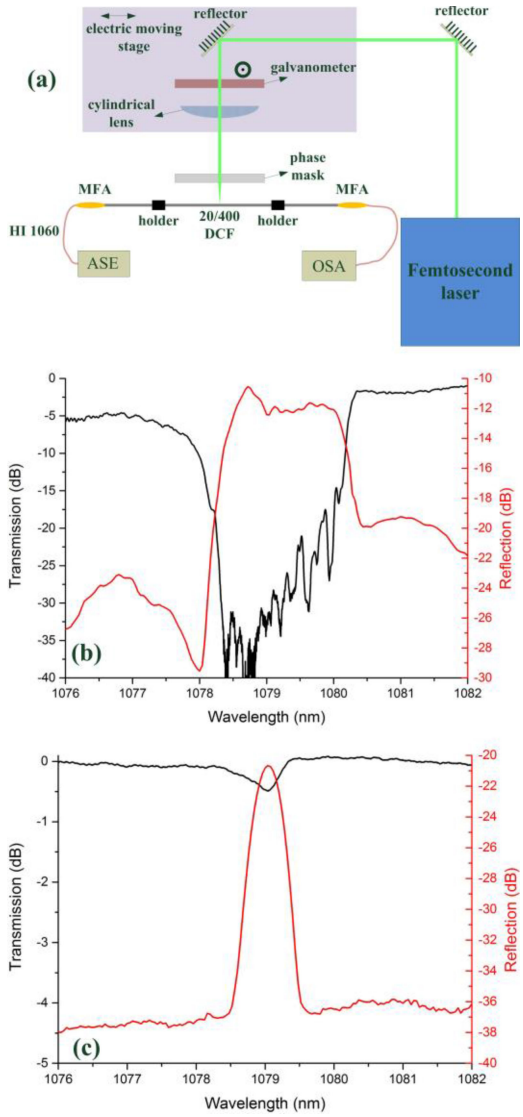

Fig. 1. (a) Schematic of femtosecond laser phase scanning system. Transmission and reflection spectrum of (b) HR-FBG and (c) LR-FBG.

Fig. 1(b) and (c) illustrate the transmission and reflection spectra of HR-FBG and LR-FBG. The length of HR-FBG is 4 cm, the bandwidth is 1.6 nm, and the reflection is higher than 99%. During HR-FBG inscription, the electrical moving stage translates in the direction of fiber axis and the galvanometer sweeps in the meaning time. The inscription of LR-FBG is much simple. We only run the galvanometer and keep the electrical moving stage still. The length of LR-FBG is only 3 mm (beam size of femtosecond laser), the bandwidth is 0.3 nm and the reflection is about 10%. Laser damage is not observed in experiment, and the insertion loss of FBGs is less than 0.03 dB. Hydrogen loading and thermal annealing are not necessary in fabrication process, and the yield of FBG also improves comparing with UV exposure method. The thermal stability is tested by setting FBGs in a heating furnace (85 °C) for 72 hours, and the spectrum before and after thermal test presents little difference.

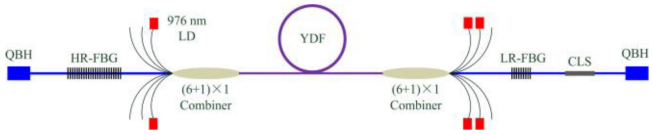

Fig. 2. Schematic of high power fiber oscillator.

III. All-Fiber High Power Oscillator

The architecture of high power fiber oscillator is shown in Fig. 2. Bidirectional-pumped scheme is carried out. In order to absorb as much pump power as possible, we use ~17 m YDFs (Nufern YDF 20/400, absorption efficiency: ~1.26 dB/m @976 nm). The YDFs are coiled in circles on water-cooling plate, and the diameter of inner circles is ~8.5 cm and that of outer circles is ~10.5 cm. The pumping source is 976 nm laser diodes (LDs), and the maximum power is ~850 W. The pump power is injected into the oscillator through two $(6 + 1) \times 1$ signal/pump combiners, which consist of one signal port and six pump ports. The pump port is with core/inner cladding of 220/242 μm and the signal port is with core/inner cladding 20/400 μm (NA: 0.065/0.46). Two pump ports of co-pumping combiner and four pump ports of counter-pumping combiner are employed. HR-FBG and LR-FBG are spliced with the signal port of co-pumping and counter-pumping combiners respectively, thus two FBGs, which are simply fixed on water-cooling plate without any special package, mainly endure the signal power. To eliminate facet reflection, we splice quartz block head (QBH) on the pigtailed fiber of two FBGs. A cladding light stripper (CLS) is applied to dump the residual pump.

The relationship between the output power and the pump power is shown in Fig. 3(a). The output power goes up linearly with the pump power, and the slope efficiency is 77.9%. During experiment, the counter-pumping power is injected into the oscillator firstly. When the counter-pumping reached its highest power 3060 W, the output power is 2368 W. Then we inject 1110 W co-pumping power, the output power reaches 3231 W. No obvious evidence of output power or efficiency decline is observed in Fig. 3(a). Fig. 3(b) demonstrates the temporal domain signal and corresponding frequency domain spectrum (the inset) at the operation of 3231 W. No drastic fluctuation is observed in the temporal domain signal and no characteristics frequency occurs in the frequency domain spectrum, which indicates that TMI effect does not occur at the output power of 3231 W. As femtosecond laser inscription can generate defects such as color centers in the glass matrix, which absorb the signal light. The temperature of FBG goes up in high power laser environment. What has to be pointed out is that the temperature of HR-FBG and LR-FBG are 40 °C and 42 °C respectively. The temperature shift is only about 20 °C. Thus, the maximum output power is only limited by pump power. Cause there still exist pump ports unoccupied, the output power can be further scaling.

The laser spectra at different output power are depicted in Fig. 4. The oscillator operates at ~1079.5 nm, which is larger than the resonant wavelength of LR-FBG in Fig. 1(b) for the heat induced resonant wavelength shift during laser output. Obviously, the laser spectra broaden drastically with the output

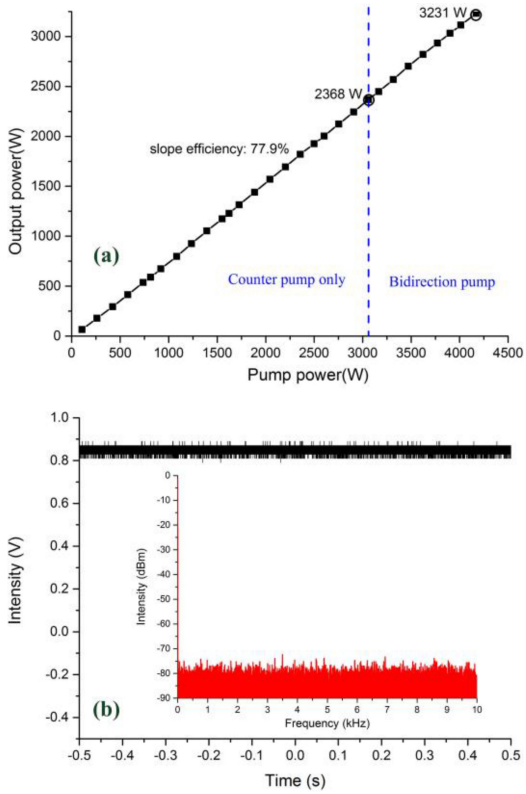

Fig. 3. (a) Relationship between output power and pump power and (b) Temporal domain signal at the operation of 3231 W.

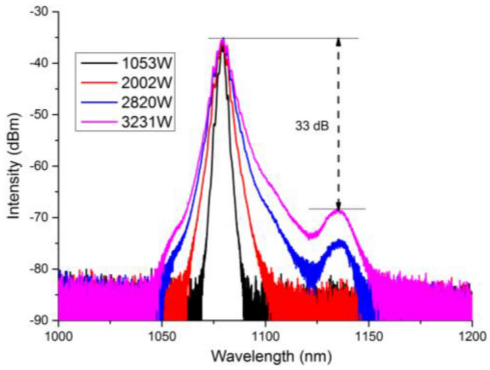

Fig. 4. Spectra under different output power.

power scaling. At the operation of 1053 W, the full width at half-maximum (FWHM) bandwidth of the laser is ~2.1 nm. When the output power reaches 3231 W, the FWHM bandwidth is ~5.5 nm. The broadening of laser spectra is contributed by the fiber nonlinear effects like self-phase modulation (SPM). Besides, when the output power increases to 2820 W, Raman-Stokes light occurs near 1135 nm. The intensity of Raman-Stokes light grows up smoothly with the output power, and it is around 33 dB below the laser intensity at the operation of 3231W.

The beam quality of the oscillator at different operation power is illustrated in Fig. 5. The M^2 factor fluctuates around 1.30 in the power scaling. The insets in Fig. 5 indicate the beam profile at the output power of 1053 W, 2002 W and 3231 W. It is obvious

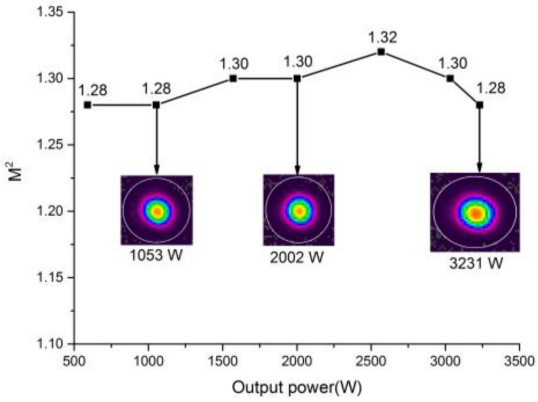

Fig. 5. Beam quality variation at different operation power.

that the oscillator works at near single mode output state even when the output reaches 3231 W. Cause 20/400 LMA-DCFs can support two core modes (LP_{01} and LP_{11}), LP11 mode does not oscillate in the laser cavity. By improving the state of splicing points in the oscillator, the beam quality can be further refined.

IV. Conclusion

In conclusion, we fabricate a pair of FBGs with resonant wavelengths near 1080 nm using visible femtosecond laser phase mask scanning technique for the first time. The usage of visible femtosecond laser simplifies the alignment process before grating inscription, and the pulse energy can be decreased for a smaller diffraction limit. A 3.2 kW near single mode output fiber oscillator is then realized by using this pair of FBGs as cavity mirrors. The slope efficiency is 77.9% and no evidence of TMI effect occurs during power scaling process. The intensity of Raman-Stokes light is 33 dB below the laser intensity at the operation of 3231 W. The FBGs pair is simply fixed on a water-cooling plate without special package, and the temperature of FBGs is around 40 °C at the maximum output power. The output power can be further scaling by increasing pump power. This work demonstrates the reliability of visible femtosecond laser in high power oscillator used FBGs fabrication. Comparing with the conventional UV exposure method, femtosecond laser inscribed FBG possesses better temperature characteristics, and can avoid cumbersome process like hydrogen loading and thermal annealing during fabrication. In the future, femtosecond laser inscribed FBG will gradually substitute the UV engraving FBG, and the output power will thus increase. Moreover, the inscription of FBG in rear-earth doped fiber becomes possible using femtosecond laser, and monolithic high power fiber lasers without splicing points will be realized.

References

[1] C. Jauregui, J. Limpert, and A. Tünnermann, "High-power fibre lasers," *Nature Photon.*, vol. 7, no. 11, pp. 861–867, 2013.

[2] Y. Xiao, F. Brunet, M. Kanskar, M. Faucher, A. Wetter, and N. Holehouse, "1-kilowatt CW all-fiber laser oscillator pumped with wavelength-beam-combined diode stacks," *Opt. Exp.*, vol. 20, no. 3, pp. 3296–3301, 2012.

[3] Y. Mashiko, H. K. Nguyen, M. Kashiwagi, T. Kitabayashi, K. Shima, and D. Tanaka, "2 kW single-mode fiber laser with 20-m long delivery fiber and high SRS suppression," in *Proc. Fiber Lasers XIII: Technol., Syst., Appl.*, 2016, Art. no. 972805.

[4] B. Yang *et al.*, "Monolithic fiber laser oscillator with record high power," *Laser Phys. Lett.*, vol. 15, 2018, Art. no. 075106.

[5] K. Shima, S. Ikoma, K. Uchiyama, Y. Takubo, M. Kashiwagi, and D. Tanaka, "5-kW single stage all-fiber Yb-doped single-mode fiber laser for materials processing," in *Proc. SPIE*, 2018, Art. no. 10512.

[6] Y. Wang *et al.*, "8-kW single-stage all-fiber Yb-doped fiber laser with a BPP of 0.50 mm-mrad," in *Proc. Fiber Lasers XVII: Technol. Syst.*, 2020, Art. no. 1126022.

[7] M. Wang *et al.*, "Fabrication of chirped and tilted fiber Bragg gratings and suppression of stimulated Raman scattering in fiber amplifiers," *Opt. Exp.*, vol. 25, no. 2, pp. 1529–1534, 2017.

[8] M. Wang, Z. Wang, L. Liu, Q. Hu, H. Xiao, and X. Xu, "Effective suppression of stimulated Raman scattering in half 10 kW tandem pumping fiber lasers using chirped and tilted fiber Bragg gratings," *Photon. Res.*, vol. 7, no. 2, pp. 167–171, 2019.

[9] V. Scarnera, F. Ghiringhelli, A. Malinowski, C. A. Codemard, M. K. Durkin, and M. N. Zervas, "Modal instabilities in high power fiber laser oscillators," *Opt. Exp.*, vol. 27, no. 4, pp. 4386–4403, 2019.

[10] W. Gao *et al.*, "Instability transverse mode phase transition of fiber oscillator for extreme power lasers," *Opt. Exp.*, vol. 27, no. 16, pp. 22393–22407, 2019.

[11] H. Li, X. Zhao, B. Rao, M. Wang, and Z. Wang, "Building-up and suppression of cladding mode coupling in fiber Bragg gratings," *J. Opt.*, vol. 22, 2020, Art. no. 075704.

[12] M. Wang, Z. Li, L. Liu, Z. Wang, X. Gu, and X. Xu, "Fabrication of chirped and tilted fiber Bragg gratings on large-mode-area doubled-cladding fibers by phase-mask technique," *Appl. Opt.*, vol. 57, no. 16, pp. 4376–4380, 2018.

[13] X. Tian *et al.*, "Influence of Bragg reflection of chirped tilted fiber Bragg grating on Raman suppression in high-power tandem pumping fiber amplifiers," *Opt. Exp.*, vol. 28, no. 13, pp. 19508–19517, 2020.

[14] K. Jiao, J. Shu, H. Shen, Z. Guan, F. Yang, and R. Zhu, "Fabrication of kW-level chirped and tilted fiber Bragg gratings and filtering of stimulated raman scattering in high-power CW oscillators," *High Power Laser Sci. Eng.*, vol. 7, 2019, Art. no. 02000e31.

[15] J. Thomas *et al.*, "Cladding mode coupling in highly localized fiber Bragg gratings: Modal properties and transmission spectra," *Opt. Exp.*, vol. 19, no. 1, pp. 325–341, 2011.

[16] H. Li, X. Zhao, B. Rao, M. Wang, B. Wu, and Z. Wang, "Fabrication and characterization of line-by-line inscribed tilted fiber Bragg gratings using femtosecond laser," *Sensors*, vol. 21, 2021, Art. no. 6237.

[17] L. Lei *et al.*, "Miniature Fabry-Perot cavity based on fiber Bragg gratings fabricated by fs laser micromachining technique," *Nanomaterials*, vol. 11, 2021, Art. no. 2505.

[18] P. Lu *et al.*, "Plane-by-plane inscription of grating structures in optical fibers," *J. Lightw. Technol.*, vol. 36, no. 4, pp. 926–931, 2018.

[19] M. L. Åslund *et al.*, "Optical loss mechanisms in femtosecond laser-written point-by-point fibre Bragg gratings," *Opt. Exp.*, vol. 16, no. 18, pp. 14248–14254, 2008.

[20] R. J. Williams, N. Jovanovic, G. D. Marshall, G. N. Smith, M. J. Steel, and M. J. Withford, "Optimizing the net reflectivity of point-by-point fiber Bragg gratings: The role of scattering loss," *Opt. Exp.*, vol. 20, no. 12, pp. 13451–13456, 2012.

[21] J. Thomas, E. Wikszak, T. Clausnitzer, U. Fuchs, U. Zeitner, and S. Nolte, "Inscription of fiber Bragg gratings with femtosecond pulses using a phase mask scanning technique," *Appl. Phys. A: Mater. Sci. Process.*, vol. 86, pp. 153–157, 2006.

[22] A. Halstuch, A. Shamir, and A. A. Ishaaya, "Femtosecond inscription of fiber Bragg gratings through the coating with a low-NA lens," *Opt. Exp.*, vol. 27, no. 12, pp. 16935–16944, 2019.

[23] J. He *et al.*, "Inscription and improvement of novel fiber Bragg gratings by 800 nm femtosecond laser through a phase mask," in *Proc. Asia Pacific Opt. Sensors Conf.*, 2016, Paper Th4A.11.

[24] R. G. Krämer *et al.*, "Femtosecond written fiber Bragg gratings in ytterbium-doped fibers for fiber lasers in the kilowatt regime," *Opt. Lett.*, vol. 44, no. 4, pp. 723–726, 2019.

[25] R. G. Krämer *et al.*, "Extremely robust femtosecond written fiber Bragg gratings for an ytterbium-doped fiber oscillator with 5 kW output power," *Opt. Lett.*, vol. 45, no. 6, pp. 1447–1450, 2020.